Comparative cranio-mandibular myology of three species of Batoidea from the Southern Gulf of California, Mexico

Article *in* Journal of Morphology · January 2023

DOI: 10.1002/jmor.21547

4 authors, including:

Rui Diogo
Howard University
358 PUBLICATIONS **5,244** CITATIONS

SEE PROFILE

Received: 4 April 2022 | Revised: 28 November 2022 | Accepted: 8 December 2022

DOI: 10.1002/jmor.21547

RESEARCH ARTICLE

JOURNAL OF morphology WILEY

Comparative cranio-mandibular myology of three species of Batoidea from the Southern Gulf of California, Mexico

Cristina Ramírez-Díaz[1] | Renato Peña[1] | Rui Diogo[2] | Víctor H. Cruz-Escalona[1]

[1]Instituto Politécnico Nacional, Centro Interdisciplinario de Ciencias Marinas, La Paz, Baja California Sur, México

[2]Department of Anatomy, Howard University College of Medicine, Washington, District of Columbia, USA

Correspondence
Renato Peña, Instituto Politécnico Nacional, Centro Interdisciplinario de Ciencias Marinas, 23096 La Paz, BCS, México.
Email: rpenam@ipn.mx

Funding information
Consejo Nacional de Ciencia y Tecnología

Abstract

The mandibular apparatus of batoids (skates, electric rays, guitarfishes, stingrays, and sawfishes) is composed of a few skeletal elements to which the muscular bundles, responsible for all movements involved in the feeding mechanism, are inserted. The description of the different mandibular morphologies can help to understand the different feeding guilds in this group. In this study, we examined the cranio-mandibular myology of adult *Rostroraja velezi*, *Narcine entemedor*, and *Zapteryx exasperata*, three species of rays that coexist in the Southern Gulf of California, Mexico. This study described the muscles on the ventral and the dorsal surfaces for each species, identified the origins and insertions of these muscles, as well as the general characteristics of muscle morphology. There were 17 and 18 muscle bundles attached to the feeding apparatus, including five on the dorsal surface. Only the levator rostri, which elevates the rostrum during feeding, showed considerable differences in shape and size among species. The muscles of the adductor complex showed the greatest differences in size among the three species. *N. entemedor* presented the exclusive muscle X in the lower mandibular area and the extreme reduction of the coracohyoideus in the pharyngeal area derived from the absence of the basihyal cartilage. The information generated in our study supports the morphological specialization of electric rays (*N. entemedor*) for an almost exclusive suction feeding strategy.

KEYWORDS
Batoids, jaws, mandibular musculature, neurocranium

1 | INTRODUCTION

Batoids (skates, electric rays, guitarfishes, stingrays, and sawfishes) are a diverse group of elasmobranchs, evolving from shark-like ancestors almost 200 million years ago (Weigmann, 2016; Whitenack et al., 2022). The characteristic dorsoventral compression of the batoid body causes the displacement of the mouth and gill openings toward the ventral surface of the body (except in Mobulidae, whose mouth is terminal); this morphology also increased the kinesis of the articulation among the jaws and the neurocranium, and facilitated the evolution of a diversity of feeding mechanisms (Aschliman et al., 2012; Dean et al., 2005; Wilga, 2002).

The feeding apparatus of the batoids consists of a few cartilaginous elements, i.e., the neurocranium, the paired upper and lower jaws (palatoquadrate and Meckel's cartilage, respectively), and the hyoid arch (with the paired hyomandibulae, a basihyal and pseudohyals; Miyake & McEachran, 1991; Nishida, 1990). The neurocranium is the structure that protects the brain and the main sensory organs. In non-Myliobatiform batoids, the anterior part of the neurocranium expands to become a rostral cartilage, which consists of an axis and an appendix, always located at the tip of the rostrum.

There is wide variability in size and shape of these rostral areas; e.g., in Rajiformes it may be fused to the rostral axis of the neurocranium (between the olfactory capsules) or just the rostral appendix without axis (Miyake et al., 1992); in Torpediniformes, the rostral appendix has irregular lateral projections, which come to articulate to the antorbital cartilage (Nishida, 1990). The stiff rostrum lacks the insertion of the pectoral fins, which facilitates their role in obtaining food when used as a paddle to strike prey, as well as to clean the sand that covers them (Wilga et al., 2012).

Regardless of the shape of the neurocranium, there are different types of mandibular suspension in the elasmobranchs (Maisey, 1980; Wilga, 2002). The mandibular suspension is classified according to the insertion of the ligaments connecting the palatoquadrate to the neurocranium: i.e., hyostylic (articulation by an ethmopalatine ligament, between the palatoquadrate and the ethmoid region of the neurocranium), orbitostylic (palatoquadrate articulates with the orbital wall of the cranium by a long orbital process) and euhyostylic (the jaws are suspended solely by the hyomandibulae without other ligaments or articulations and the hyoids arch are modified). This last type of suspension is exclusive of the batoids; because no ligament connects the neurocranium with the jaws, the hyomandibular cartilages are responsible for this union, and it also causes the pseudoceratohyal-basihyal union to be associated with the first gill arch instead of the hyomandibular cartilage (Motta & Huber, 2012; Wilga, 2002, 2008; Wilga & Motta, 1998). Euhyostyly is thought to permit a greater range of upper and lower jaw motions during feeding (Dean & Motta, 2004b; Dean et al., 2005; Wilga et al., 2007; Wilga, 2008).

The muscle complexity and arrangement caused by the euhyostylic suspension is partially responsible for the ecological diversity observed in batoids. The combined action of the different muscle bundles and, the type of dentition, results in a diversity of feeding mechanisms, including generalist predators of vertebrate and invertebrates (Jacobsen & Bennett, 2013; Navarro-González et al., 2012; Simental, 2013); filter feeders specialized in consuming krill (McEachran & Capape, 1984; Notarbartolo-di-Sciara,1987; Paig-Tran et al., 2013; Sampson et al., 2010), and even durophagous predators, which crush mollusks and other shelled invertebrates (Collins et al., 2007; Gray et al., 1997); these predators also require other types of modifications such as the thickening of the jaws and the insertion and articulation ligaments, as they need to separate the edible components from the inedible ones (Dean et al., 2005, 2007; Kolmann et al., 2014, 2016; Motta & Huber, 2012; Sasko et al., 2006; Wilga & Motta, 1998).

The morphological descriptions of the mandibular apparatus of batoids developed over the years have been of great importance for the understanding of the feeding ecomorphology of the group (Dean et al., 2005, 2007; Kolmann et al., 2016; Sasko et al., 2006; Wilga & Motta, 1998; Wilga, 2002). However, most of these works have been focused on durophagous species belonging to the Myliobatidae family, which is a group of great interest due to the anatomical specializations they exhibit like the thickening and calcification of the mandibular cartilages (Summers, 2000), the organization of the tendon tissue which is similar to that present in mammals (Summers & Koob, 2002), the shape and size of the mandibular muscles responsible for the bite and the adductors showing an increase in size (González-Isáis & Domínguez, 2004; González-Isáis, 2003; Kolmann et al., 2014). Many studies focused on the contribution of muscle architecture to the bite force in myliobatid rays and the correspondence with their ability to regulate the force and leverage of the jaws (Kolmann et al., 2015, 2018; Sasko et al., 2006). There were also morphological studies in nondurophagous species, which described the general morphology of the mandibular apparatus and the elements that compose it (Nishida, 1990). Also, the muscular activity during different phases of the feeding has been described, either during bite and jaw protrusion in *Rhinobatos lentiginosus* (Wilga & Motta, 1998), at the moment of mandibular protrusion in *Narcine brasiliensis* (Dean & Motta, 2004a, 2004b) or the modulation of the mandibular musculature in *Leucoraja erinacea* (Gerry et al., 2010) and *Dasyatis sabina*, *Gymnura micrura*, *Potamotrygon motoro*, and *Urobatis halleri* (Gerry et al., 2019).

Morphological studies are important to understanding the biology of any organism. Particularly in batoids, the morphological analysis of the mandibular muscle bundles, understanding the variation in their organization in different species and the action of each mandibular muscle during the feeding process could provide a clearer evolutionary interpretation of the dietary diversity and the ecomorphological feeding relationships within the habitat in which the species are found. Together with current molecular studies, this approach may also provide a better phylogenetic understanding of the group. Therefore, the objective of the present study was to generate morphological information of the mandibular apparatus in non-durophagous species of batoids, the banded guitarfish *Zapteryx exasperata*, the giant electric ray *Narcine entemedor*, and the rasptail skate *Rostroraja velezi*, which are distributed in the southern Gulf of California and will contribute to our understanding of the evolution of different feeding mechanisms in batoids.

2 | MATERIALS AND METHODS

The specimens were collected by local independent fishermen from the Bay of La Paz, BCS, Mexico. The specimens were euthanized in the field according to the Report of the AVMA Panel on Euthanasia. American Veterinary Medical Association (2001) making a cut in the spinal cord, close to the neurocranium and were preserved in a freezer (−20°C). After 10 days, the specimens were immersed in 10% buffered formalin for 15 days and then washed with tap water and preserved permanently in 70% ethanol. The analysis was realized on adult specimens of *Rostroraja velezi* (Chirichigno, 1973) ($n = 6$) with a disk width (DW) of 57–67; *Narcine entemedor entemedor* (Jordan & Starks, 1895) ($n = 7$) with a DW of 26–35 cm; and *Zapteryx exasperata* (Jordan & Gilbert, 1880) ($n = 7$) with a DW of 32–35 cm.

The mandibular musculature of all the specimens was exposed by removing the skin from the dorsal and ventral surface of the cephalic region. For descriptive purposes, the myological analysis of the

ventral surface was performed on four levels of dissection, which do not represent the developmental groupings of the muscle bundles. During the dissection process, several photographs were taken with a digital camera (Nikon D3200). Illustrations from each photograph were prepared by using a digital drawing tablet (Wacom One Small) and the Paint Tool SAI software for Windows. Muscles were identified by considering both the attachment points (origin and insertion) as well as the general location of the muscle bundle within the head. Considering that there is variable terminology used in the mandibular myology of rays (Table 1), the present study uses the terminology of Wilga & Motta (1998); Dean & Motta (2004a) and Kolmann et al. (2014).

3 | RESULTS

The muscles of the cranio-mandibular region of the analyzed species followed the general body pattern of batoids, i.e., 17 or 18 muscles that are engaged in the feeding process, most of them located on the ventral surface of the organism. To facilitate localization and description, each muscle bundle in the cephalic area has been described with reference to its area of origin and insertion (Table 2).

3.1 | Neurocranium

The species analyzed had a simple skull, endowed with elongated rostral cartilage that extended from the anterior limit of the olfactory capsules toward the anterior part of the body, giving shape to the rostrum. In *R. velezi* and *Z. exasperata*, the rostral axis of this cartilage was narrower than the rest of the neurocranium (Figure 1a and 1c, respectively), with a widening at the tip, i.e., the rostral appendix. In *N. entemedor*, the neurocranium and rostral cartilage adopted an almost rectangular shape along their entire length (Figure 1b).

The three species studied had more than one fontanelle: *Z. exasperata* and *N. entemedor* had two and *R. velezi* had three. In *Z. exasperata* and *N. entemedor*, the posterior cranial fontanelle was

TABLE 1 Cranial structures and mandibular musculature in batoids

Abbreviation	Structure	Abbreviation	Musculature division
ACF	Anterior cranial fontanelle	AMLa	*Adductor mandibulae lateralis*
ANT	Antorbital cartilage	AMMa	*Adductor mandibulae major*
ARF	Anterior rostral fossa	AMMe	*Adductor mandibulae medialis*
BH	Basihyal cartilage	CARC	*Coracoarcualis*
EPB	Epiphyseal bridge	CH	*Coracohyoideus*
EYB	Eyeball	CHD	*Constrictor hyoideus dorsalis*
Fsc	Fascia	CHV	*Constrictor hyoideus ventralis*
HYM	Hyomandibular cartilage	CHYM	*Coracohyomandibularis*
HYBC	Hypobranchial cartilage	CM	*Coracomandibularis*
Lab	Labial cartilage	DBL	Dorsal longitudinal muscles
MCF	Middle cranial fontanelle	DHYM	*Depressor hyomandibularis*
MK	Meckel's cartilage	DM	*Depressor mandibularis*
NC	Neurocranium	DR	*Depressor rostri*
OLF	Olfactory capsule	LHYM	*Levator hyomandibularis*
OTC	Otic capsule	LP	*Levator palatoquadrati*
PCF	Posterior cranial fontanelle	LR	*Levator rostri*
POP	Postorbital process	SB	*Suborbitalis*
PQ	Palatoquadrate cartilage	SP	*Spiracularis*
PRF	Posterior rostral fossa	X	Muscle X
PREP	Preorbital process		
PROP	Propterygium		
RAP	Rostral appendix		
RAX	Rostral axis		
RC	Rostral cartilage		

TABLE 2 Dorsal and ventral cranial musculature in *Rostroraja velezi*, *Narcine entemedor*, and *Zapteryx exasperata*

Position/level	Muscle	Abbrev.	Origin	Insertion
Dorsal	*Levator rostri*	LR	Perpendicular to synarcual/dorsal neurocranium	Propterygium/antorbital cartilage
Dorsal	*Levator hyomandibularis*	LHYM	Otic capsule of the neurocranium	Hyomandibular cartilage
Dorsal	*Spiracularis*	SP	Lateral surface of the neurocranium	Spiracular cartilage, hyomandibular cartilage, external oropharyngeal tissue
Dorsal	*Levator palatoquadrati*	LP	Neurocranium (otic capsule)	Palatoquadrate cartilage
Dorsal	Dorsal longitudinal bundles	DLB	Scapular girdle	Neurocranium/otic capsules
Ventral/N1	*Depressor rostri*	DR	Midline of the body	External border of the rostrum
Ventral/N2	*Suborbitalis*	SB	Neurocranium	Meckel's cartilage
Ventral/N2	*Adductor mandibulae major*	AMMa	Palatoquadrate cartilage	Meckel's cartilage
Ventral/N2	*Depressor mandibulae*	DM	Dorsal surface of *depressor rostri*	Meckel's cartilage
Ventral/N2	Muscle X	X	Hyomandibular cartilage	Ligamentous sling of Meckel's cartilage
Ventral/N2	*Coracomandibularis*	CM	*Coracoarcualis*	Meckel's cartilage
Ventral/N2	*Coracoarcualis*	CARC	Scapular girdle	*Coracomandibularis*
Ventral/N3	*Adductor mandibulae lateralis*	AMLa	Palatoquadrate cartilage	Meckel's cartilage
Ventral/N3	*Adductor mandibulae medialis*	AMMe	Palatoquadrate cartilage	Meckel's cartilage
Ventral/N3	*Depressor hyomandibularis*	DHYM	*Coracomandibularis*	Hyomandibular cartilage
Ventral/N3	*Coracohyoideus*	CH	Second fascia	Basihyal cartilage
Ventral/N3	*Constrictor hyoideus ventralis/ dorsalis*	CHV/CHD	Septum medial of the first branchial arch	Ventral/dorsal first branchial arch
Ventral/N4	*Coracohyomandibularis*	CHYM	Midline of the body	Hyomandibular cartilage

Note: N1, first dissection level; N2, second dissection level; N3, third dissection level; N4, fourth dissection level.

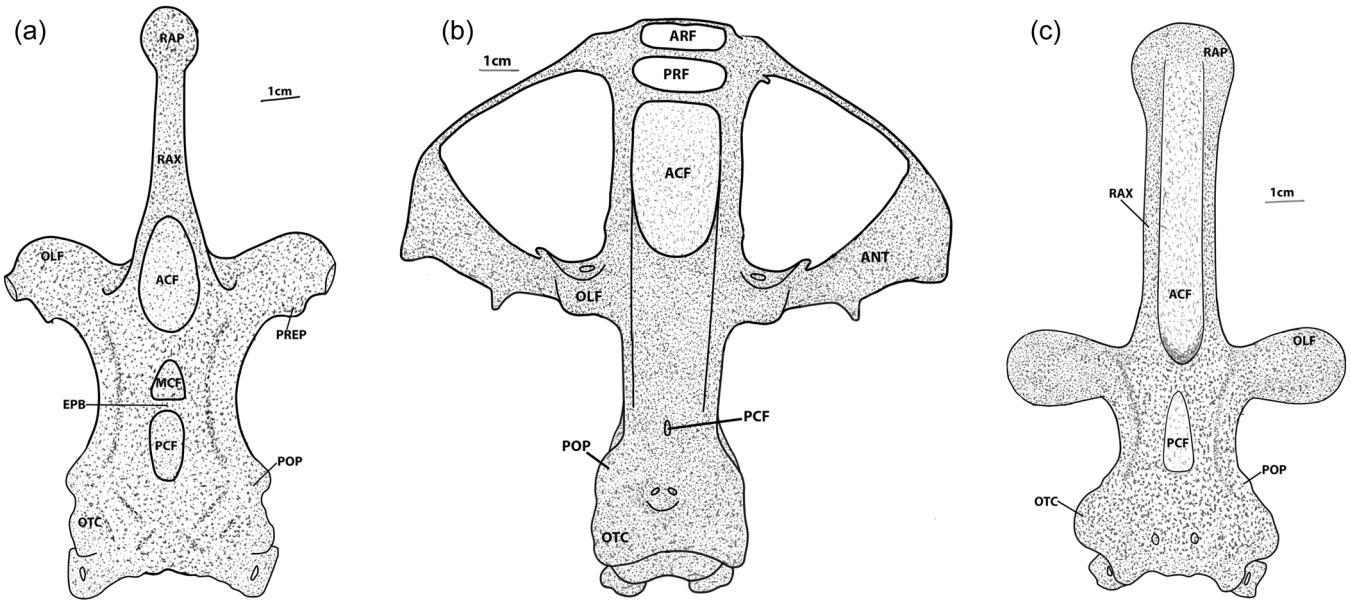

FIGURE 1 Dorsal view of the neurocranium in three batoid species: (a) *Rostroraja velezi*, (b) *Narcine entemedor*, and (c) *Zapteryx exasperata*

small, with an almost oval form, and located on the cranial box, and the anterior cranial fontanelle was located practically along the entire length of the rostral cartilage. In *R. velezi*, the middle and posterior cranial fontanelles were located on the neurocranium, separated by the epiphyseal bridge and the anterior cranial fontanelle was located at the base of the rostral cartilage (Figure 1a). In addition, *N. entemedor* showed two rostral fossae, located on the top of the rostral cartilage, and a pair of antorbital cartilages whose posterior portions were attached to the olfactory capsules, while the anterolateral portions were connected to the rostral cartilage by a network of tissue, providing the characteristic rounded shape of the electric rays (Figure 1b).

3.2 | Dorsal mandibular muscles

3.2.1 | Levator rostri (LR)

The LR was variable in size and shape depending on the species and was located between the gill arches and the otic capsule of the neurocranium. It had two zones of origin, which differed according to species. In *R. velezi and Z. exasperata*, the first origin (origin A) or posterior zone of the muscle was located parallel to the vertebral column, at the posterior-internal border of the third gill arch for *Z. exasperata* and below the fifth arch in *R. velezi*. The second point of attachment (origin B) was located below the hyomandibular by a small tendon (Figure 2a and 2c). In *N. entemedor*, origin A was in the dorso-caudal portion of the otic capsule, from the border of the dorsal longitudinal bundles (DLB), at the level of the third branchial arch and over the hyoid arch. Origin B was by a tendon on the lateral surface of the neurocranium below the levator palatoquadrati (LP; Figure 2b).

The muscle insertion occurred via a long and rounded tendon, located at the external limit of the hyomandibulae. In *R. velezi and Z. exasperata* (Figure 2a and 2c), it extended from the medial height of the levator hyomandibularis (LHYM) to the anterior border of the rostrum, over the middle of the adductor mandibulae major (AMMa). In *N. entemedor* (Figure 2b), the LR had two points of insertion: The first occurred via a series of connective tissue fibers along the outer dorso-lateral surface of the neurocranium, slightly surrounding the eyeball. The second and larger insertion point occurred via a long and rounded tendon inserted into the external limit of the antorbital cartilage (Figure 2b). In *N. entemedor*, the LR was extremely broad, covering most of the dorsal musculature.

3.2.2 | Levator hyomandibularis (LHYM)

The origin of the LHYM was observed on the entire lateral external surface of the otic capsule of the neurocranium, from the posteroventral border of the postorbital process (when present), to the posterior limit of the neurocranium, at the level of the occipital condyles. The insertion was located at the dorsolateral surface of the hyomandibular cartilage, up to the edge of the articulation with the jaw, on the dorsal surface, below the spiracularis (SP), via a wide tendon running from the external border of the postorbital process to the external border of the hyomandibular cartilage. The LHYM was composed of flattened fibers, located in the three species and forming the hyomandibula portion of the buccopharynx. It was located over the entire surface of the hyomandibular cartilage (Figure 2).

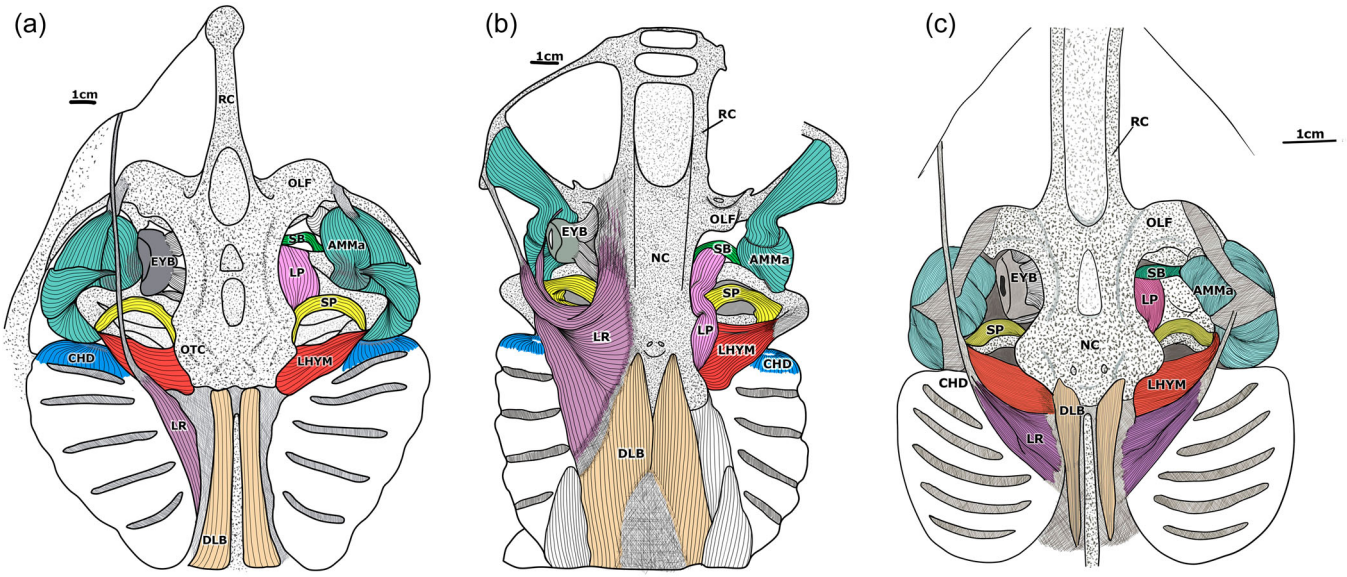

FIGURE 2 Dorsal superficial cephalic musculature of three batoid species: (a) *Rostroraja velezi*, (b) *Narcine entemedor*, and (c) *Zapteryx exasperata*. The left side of each image shows the entire cephalic area, including the eyeball, and the right side shows only the cephalic musculature (Table 1)

3.2.3 | Spiracularis (SP)

The origin of the spiracularis occurred on the lateral surface of the neurocranium, close to the posterior border of the otic capsule, via a small tendon connected to the foramen in the otic process. The muscle inserted below the LHYM, comprising small connective tissue fibers in two different zones. The first one (superior) was on the dorsal-internal face of the hyomandibula, reaching the articulation with the mouth, and the second zone was on the ventral surface of the external oropharyngeal tissue (the dorsal-internal surface of MK). The SP is slightly flattened muscle and was located perpendicular to the neurocranium on the spiracular cartilage covering the entire dorsal surface (Figure 2).

3.2.4 | Levator palatoquadrati (LP)

The origin of the LP extended from the lateroventral surface of the otic capsule to the surface of the floor of the neurocranium near the hyomandibular articulation (Figure 2). The insertion was located on the dorsal surface of the palatoquadrate cartilage (PQ), near the symphysis via a small tendon. This muscle was associated with the SP, and the fibers of the muscle bundle were attached to the external surface of the oropharyngeal cavity. However, in *N. entemedor* this attachment was only made with the anterior portion of the muscle; the rest of the muscular bundle was located on the dorsolateral border of the neurocranium (Figure 2b).

3.3 | Dorsal longitudinal bundles (DLB)

The DLB were located in the dorsal midline of the specimen, originating from the neurocranium and extending to the scapular girdle, parallel to the synarcual cartilage. They were bundles of variable shape and size depending on the species. In *R. velezi*, they inserted into the posterior border of the neurocranium (Figure 2a). In *N. entemedor* and *Z. exasperata* (Figure 2b,c), they inserted into the dorsal surface of the neurocranium, in the area of the otic capsules. These muscles covered a large area of the neurocranium in *N. entemedor* (Figure 2b).

3.4 | Ventral mandibular muscles

3.4.1 | Level 1

Depressor rostri (DR)

The DR extended from the midline to the lateral-external border of the face and was the most superficial muscle on the ventral surface. Its origin was similar in all species in the midline of the body, and was made by a series of connective tissue fiber. The insertion of the muscle was generally located in the external border of the rostrum by a long tendon (Figure 3). In *R. velezi* and *Z. exasperata* the DR had two insertions; the larger part of the muscle attached to the anterior border of the face, above the olfactory capsule, while the second branch was much thinner, in *R. velezi* by a thin tendon that was attached to the inferior nasal cartilage (Figure 3a) and in *Z. exasperata* this second branch was attached to the propterygium (Figure 3c). In

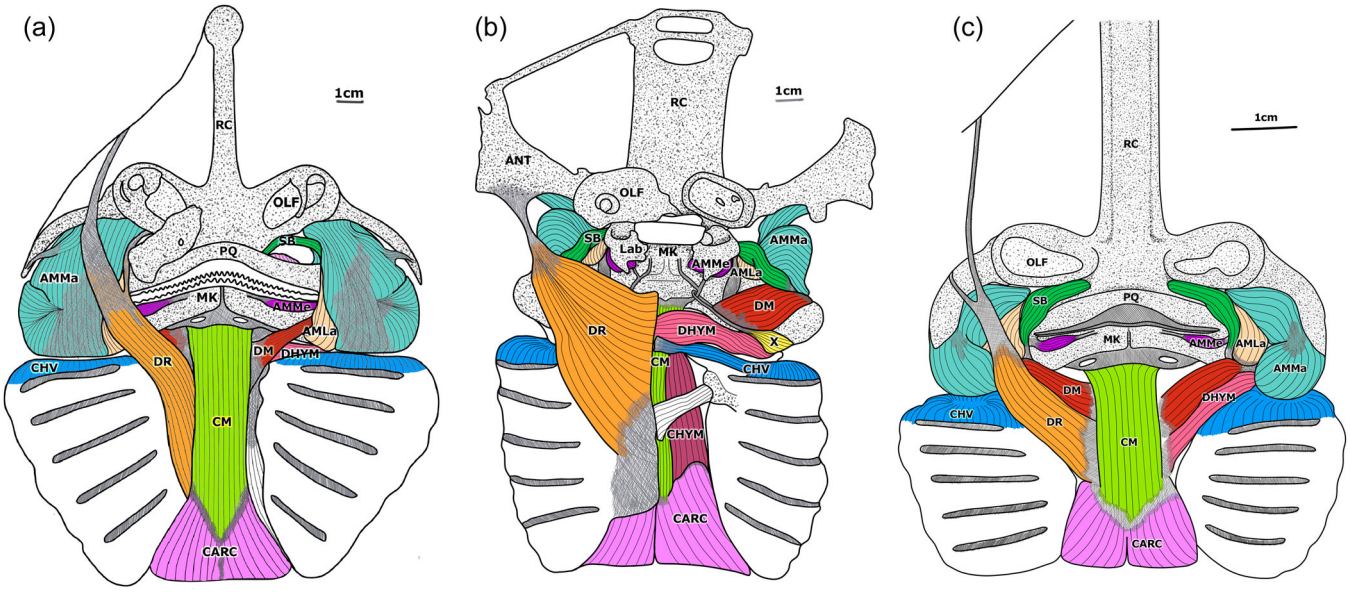

FIGURE 3 Ventral mandibular musculature of three batoid species: (a) *Rostroraja velezi*, (b) *Narcine entemedor*, and (c) *Zapteryx exasperata* The left side of each image shows the complete muscle at the first level of insertion (N1, Table 1), and the right side shows the second level of dissection (N2, Table 1)

N. entemedor, the DR was a broad muscle extending from the third branchial arch to almost the entire pharyngeal area and inserting into the antorbital cartilage (Figure 3b).

3.4.2 | Level 2

Suborbitalis (SB)

The SB was generally long and considerably thick, located on the ventral surface surrounding the buccal opening. Its origin was similar in all species: on the ventral surface of the neurocranium, posterior to the olfactory capsules by a reduced tendon. Its insertion occurred via a small tendon that connects to MK (Figure 4). In *R. velezi*, the SB was an exceptionally thin muscle whose insertion was located below the AMMa (Figures 2a and 3a). In *N. entemedor*, the insertion was located at the articulation of the PQ and MK, below the AMMa. In *Z. exasperata*, the SB surrounded the buccal aperture, and its insertion was associated with the adductor mandibulae lateralis (AMLa) (Figures 2c and 3c).

Adductor mandibulae major (AMMa)

The AMMa was the largest and most voluminous muscle of the abductor complex, with a fiber architecture organized in an "8" shape, suggesting that this muscle has multipennate fiber architecture, like in other batoids. The muscle completely covered the mandibular cartilage joint and was visible both dorsally and ventrally on the body. Therefore, it was difficult to determine a single area of origin and insertion; however, for practical purposes, the origin of the AMMa has been located on the PQ and the insertion on MK (Figures 2 and 3). This muscle had two or three divisions, which joined different mandibular and neurocranial structures, depending on the species. In *R. velezi*, the AMMa was a voluminous muscle with several defined divisions; the anterior was inserted dorsally to the propterygium, near its articulation with the olfactory capsule, via a relatively rectangularly shaped tendon and ventrally to the end of the propterygium (Figures 2a and 3a). In *N. entemedor*, this muscle was compact in its medial zone, relatively spherical in shape, with an elongated anterior division that inserted into the dorsal surface of the antorbital cartilage (Figure 2b). In *Z. exasperata*, the AMMa was rather oval-shaped muscle. The anterior division was attached to the inner surface of the propterygium, from its articulation with the olfactory capsule. In addition, the dorsal surface had an aponeurosis that connected the muscle bundle with the dorsal surface of the olfactory capsule (Figures 2c and 3c).

Depressor mandibularis (DM)

The DM varied in size and shape among the species. It originated on the dorsal surface of the DR, at the level of the lateral border of the coracomandibularis (CM), by a fibrous tissue. The insertion point was located on the ventral surface of MK, slightly covering the posterior surface of the cartilage. In *R. velezi* and *Z. exasperata*, the insertion of the DM was associated with a zone of insertional aponeurosis, shared with the SB and AMLa, near the commissure of the mouth (Figure 4a and 4c). In *N. entemedor*, the DM was a more voluminous muscle, located in the external zone of MK, close to the articulation with the PQ. Its origin was located in the inferior border of MK and was highly associated with a portion of thickened connective tissue that is part of the ligamentous sling. The ligamentous sling is a network of intertwined ligaments from the CM, muscle X, DM, and the AMLa, which was located in the medial area of the mandibular symphysis (Figures 4b and 5b).

Muscle X

Muscle X was small and present only in *N. entemedor* (Figures 4b and 5b). The muscle fibers extended in the space among the DM and the depressor hyomandibularis (DHYM), from the hyomandibular

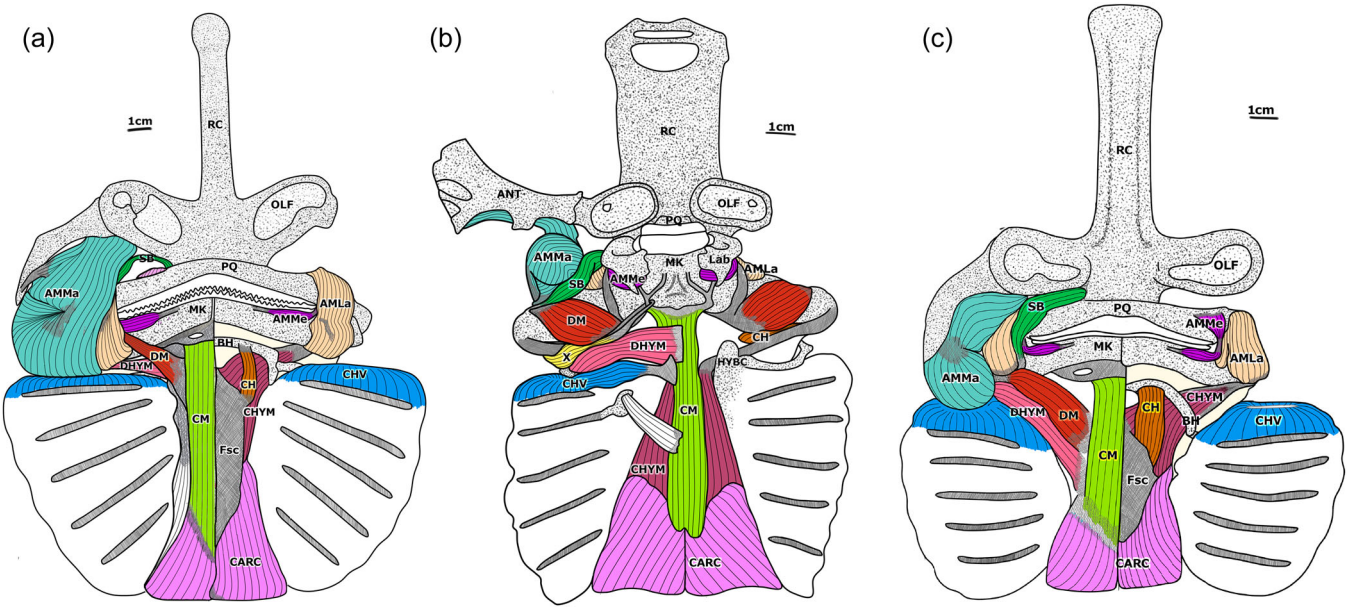

FIGURE 4 Ventral mandibular musculature of three batoid species: (a) *Rostroraja velezi*, (b) *Narcine entemedor*, and (c) *Zapteryx exasperata*. The left side of each image shows the second level of dissection (N2), and the right side shows the third level of dissection (N3) (Table 1)

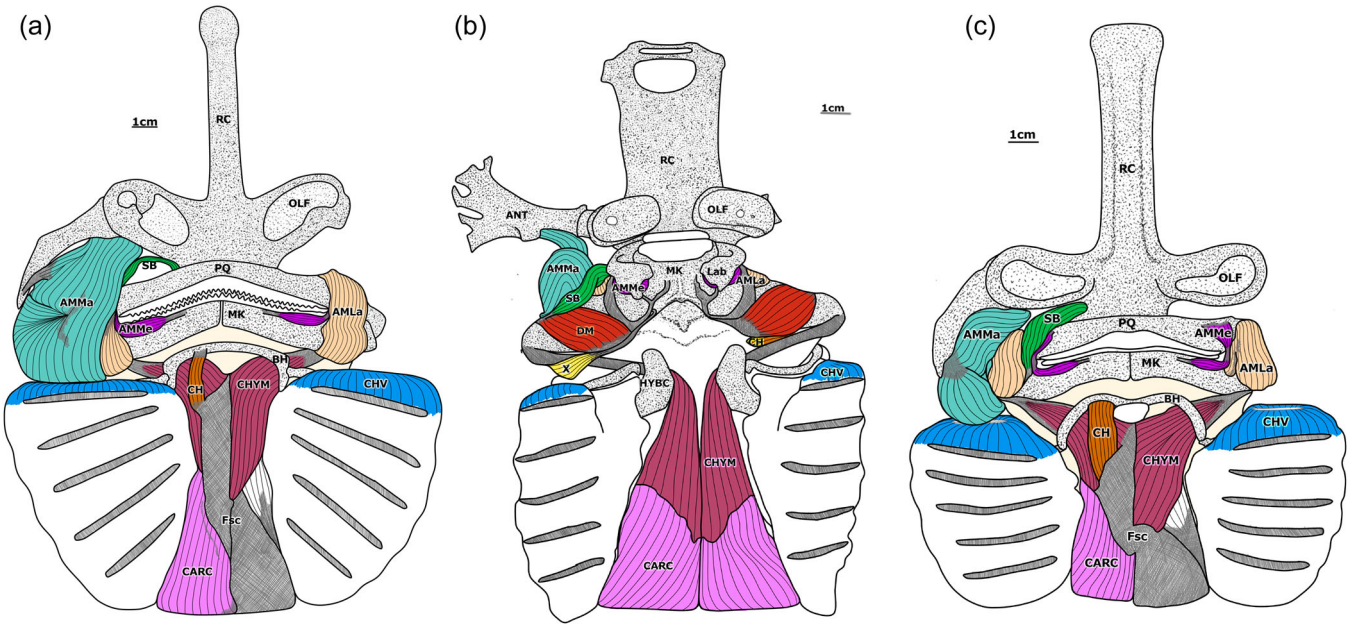

FIGURE 5 Ventral mandibular musculature of three batoid species: (a) *Rostroraja velezi*, (b) *Narcine entemedor*, and (c) *Zapteryx exasperata*. The left side of each image shows the third level of dissection (N3), and the right side shows the fourth level of dissection (N4) (Table 1)

cartilage to the medial part of MK at approximately 45°. Its origin was located below the tendon of the DHYM insertion, over the hyomandibular cartilage, near its articulation with the mandible. The insertion zone occurred in the corner of the ligamentous sling, below the bifurcation (Figure 4b).

Coracomandibularis (CM)

The CM was a long and broad muscle, almost rectangular in form and located in the medial portion of the body, extending along nearly the entire length of the esophageal tract (Figure 4). The origin was V-shaped and located in the mid-posterior part of the esophageal tract, associated with the insertion of the coracoarcualis (CARC). The insertion occurred at the posterior border of MK, below the symphysis. This muscle bundle was narrower in *N. entemedor* compared with the other species, and inserted in MK, without touching the teeth, in the ligamentous sling by thin tendons in a "Y" shape (Figure 4b).

Coracoarcualis (CARC)

The CARC comprised a voluminous pair of muscles, usually of a triangular shape, located at the limit of the posterior zone of the oropharyngeal cavity. The origin of these muscles occurred at the anterior border of the scapular girdle, on the ventral surface of the pericardium. Both bundles came into contact in the medial part of the body until their insertion point, a "V" shape at the level of the origin of the CM (Figure 4). Compared with the other species, in *N. entemedor* the CARC were slim bundles, and they did not have contact with the pericardium, because they were located on the ventral surface of the coracohyomandibularis (CHYM; Figure 4b).

3.4.3 | Level 3

Adductor mandibulae lateralis (AMLa)

The AMLa extended in the middle area of the abductor complex from the corner of the mouth to the external border of the mandible, covering the ventral surface of the articulation among the PQ and MK. Its origin occurred on the PQ, along the ventral process of the cartilage, almost at the joint. The insertion was over the inferior border of MK. In *R. velezi*, the AMLa was predominantly covered by the AMMa (Figure 4a). In *N. entemedor*, the AMLa was much smaller and covered with the SB (Figure 4b). In *Z. exasperata*, the connective tissue that inserts the AMLa was associated strongly with the insertion of the SB and DM in the inferior border of MK (Figure 4c).

Adductor mandibulae medialis (AMMe)

The AMMe was the smallest muscle of the abductor complex, generally located around the corner of the mouth, surrounding the external border of the teeth. *Rostroroja velezi* and *Z. exasperata* showed an area of fibrous tissue attached at the corner of the mouth dividing the muscle in two sections: the upper jaw section (origin) and the lower jaw section (insertion). The upper section was flattened and shaped like an inverted triangle perpendicular to the oral opening and located below the AMLa (Figure 4a and 4c). The lower section had a cylindrical shape and was in MK through a small and flattened tendon attached to the teeth. In these species, no labial cartilages associated with this muscle were observed. In *N. entemedor*, however, both sections were rectangular with similar size and the entire muscle bundle was covered by the labial cartilage (Figure 4b).

Depressor hyomandibularis (DHYM)

In *R. velezi* and *Z. exasperate*, the DHYM originated at the lateral border of the CM, on the dorsal surface of the DR or the DM, respectively (Figure 4a and 4c). In *N. entemedor*, the muscular antimeres had the same origin in the middle of the anterodorsal portion of the DR (Figure 4b). In the three species, the muscle inserted by a long tendon on the posterolateral surface of the hyomandibular cartilage, and anterior to the articulation with the mandible, but in *N. entemedor*, the insertion occurred above the insertion of muscle X in the hyomandibular cartilage (Figure 4b).

Coracohyoideus (CH)

The CH was notably small and slender, almost rectangular in shape, located parallel to the midline of the body. The origin occurred on the ventral surface of the second fascia that separates the CM + CARC complex from the CHYM, at the same level as the second branchial arch. The insertion point was on the surface of the BH (Figure 5a and 5c). In *N. entemedor*, the CH was reduced markedly, resulting from the absence of the BH in the medial area of the oropharyngeal region; in addition, the muscle bundle was located close to the hyomandibular joint, below the large tendon of insertion of the CHYM (Figure 5b).

Constrictor hyoideus ventralis (CHV) and constrictor hyoideus dorsalis (CHD)

The CHV and CHD were in the anterior zone of the hypobranchial complex, forming a barrier among this complex and the hyoid region. Both bundles (dorsal and ventral) originated from the septum medial of the surface of the first branchial arch (Figures 2–5). In *N. entemedor*, there was an elongation of the muscle fibers of the CHV, running parallel to the DHYM, from the transverse surface to the midline of the organism (Figures 3b and 4b).

3.4.4 | Level 4

Coracohyomandibularis (CHYM)

This paired muscle was located on the lateral surface of the pharyngeal area. Both antimeres were closely related in their region of origin which occurred in the medial line of the body, below the second fascia supporting the CM + CARC complex (Figure 5). The fibers of this bundle extended almost perpendicular to the midline of the body, down the lateral extensions of the BH and inserting via a strong tendon into the hyomandibular cartilage. The insertion tendon could be considered the largest of all the mandibular muscles. Particularly notable in *N. entemedor* was the cylindrical shape of the tendon of insertion; however, due to the absence of the BH, the muscle bundles stayed together in the middle of the body and the tendon ran under the first hypobranchial cartilage until reaching its insertion point (Figure 5b).

4 | DISCUSSION

The morphology of the mandibular apparatus in batoids follows a general pattern of organization that originates from the dorsoventral compression of the body, which causes the adaptation of the cartilaginous elements, the type of articulation of these elements, and the shape and organization of the muscular bundles (González-Isáis, 2003; Kolmann et al., 2014; Motta & Huber, 2012; Nishida, 1990; Wilga & Motta, 1998).

The general location of the cephalic musculature on the dorsal and ventral surfaces of *R. velezi*, *N. entemedor* and *Z. exasperata* reported in the present study is consistent with what has been described in other non-durophagous batoid species like *R. lentiginosus* (Wilga & Motta, 1998), *N. brasiliensis* (Dean & Motta, 2004a), *Potamotrygon motoro* (Shibuya et al., 2012), and in some durophagous members of the superfamily Myliobatidae (González Isáis & Montes Domínguez, 2004, 2016; González-Isáis, 2003; Kolmann et al., 2014). However, relevant differences were observed in some muscles that are important to emphasize due to their roles in some phases of the feeding process.

The presence of the LR on the dorsal surface, for example, is a unique feature in batoid species with a rostral cartilage (Kolmann et al., 2014; Miyake et al., 1992); its function is the movement of the anterior part of the rostrum or nose. Although the organization of the bundle in *N. entemedor* generally corresponds to that described previously by Dean and Motta (2004a) for *N. brasiliensis*, and therefore, could be considered as the general form for this genus, our study extends the description of the organization of the muscle fibers at the insertion point, including the section surrounding the eye. The increased insertion surface in the group may explain the long upward and downward movements of the head that electric rays exhibit during the winnowing phase (cyclic protrusion and retraction of the jaws with expulsion of inedible material) described by Dean & Motta (2004b). However, *R. velezi* presents the comparatively smallest LR among the three species studied, probably associated with the narrow rostral cartilage. Also, it is known that species with rostral cartilage use the rostrum to capture and hold the prey and its movement is restricted to this first phase of the feeding process (the capture), similar to the study by Wilga and Motta (1998) in *Rhinobatos lentiginosus*; however, it will be important investigate if the reduction of muscle fibers and the increase in the length of the insertion ligament affect the type or range of rostral movements that the Rajiformes can made.

On the ventral surface, the DR along with the LR control the rostral region of the organism during prey capture (Wilga & Motta, 1998), specifically during the end of the feeding process during "compression transport" as described by Dean and Mota (2004b). In *N. entemedor*, the large and voluminous DR moves and supports the rostrum during the retraction of the jaws, which occurs by the flexion of the antorbital cartilages where this muscle was inserted and not by direct movement of the rostral cartilage. However, it should be emphasized that not only the species with antorbital cartilages and robust rostral cartilage have a large DR, because Myliobatiform

species exhibit a larger bundle with a greater coverage of the ventral cephalic surface, although with a reduced or almost non-existent ligamentous insertion (González Isáis & Montes Domínguez, 2016; González-Isáis, 2003; Kolmann et al., 2014), suggesting that the function of depressing the rostrum is especially important for species whose jaws are highly protractile.

We report the presence of DM in all the analyzed species, which contrasts with previous studies like Kolmann et al. (2014) who did not report it in Rajiformes, or Nishida (1990) who named the DM as *intermandibularis posterior* and reported it as absent in Torpediniformes and Rajiformes. The standardization of the names might be possible considering the description and general location of the muscle bundle, specifically the insertion point that is close to the AMLa; therefore, we suggest using DM as the most appropriate name, according to the results obtained in the species analyzed. Also, the origin of DM is related to the dorsal surface of the DR and in some cases it is an extremely narrow muscle bundle, as in *R. velezi* (Figure 4c), which makes it difficult to locate it in Rajiformes. However, more studies are necessary in other representative families of Batoidea like Rajidae, Torpedinidae and Rhinobatidae to confirm the presence or absence of this muscle and therefore, the possible role as a distinctive character in the evolutionary description of the group.

The DHYM, in conjunction with other muscles like the CHYM and the DM, is responsible for the mandibular and hyoid depression and has the ability to retract the pharyngeal floor, depressing the hyomandibular cartilage, and contributing to mandibular protrusion (Dean & Motta, 2004a; Kolmann et al., 2014; Miyake et al., 1992; Wilga & Motta, 1998). Among the three studied species, *R. velezi* had the smallest DHYM, which is consistent with its feeding behavior and classification as a tertiary carnivore (Molina-Salgado et al., 2021; Simental, 2013). Indeed, this species uses biting as the most recurrent feeding mechanism and has poor or null protrusibility of the jaw. Hence, it requires greater bite force and speed, which are provided by other muscles (Summers, 2000). However, the CHYM in *N. entemedor* exhibits a prominent tendon of insertion whose size could be directly related to the increase in suction velocity and the gradual release of the compressive force that the muscle applies on the hyomandibulae (Dean & Motta, 2004a). The high protrusion velocity of the mandible may result in prey capture before the rest of the body touches the substrate. Furthermore, it has been reported that maximum suction pressures occur before the prey contacts the buccal cavity (Dean & Motta, 2004b; Svanbäck et al., 2002). The ability to sustain the force of contraction of the muscle fibers may provide the acceleration and ballistic protrusion of the jaw during the fast-opening phase (Dean & Motta, 2004a). In addition, the use of the strongest possible force in this contraction would help to transport food across the buccopharyngeal portion of the digestive tract.

Several authors (e.g., Wilga & Motta, 1998; Wilga, 2002; Dean & Motta, 2004a, 2004b; Dean et al., 2005; Gerry et al., 2019; Kolmann et al., 2014, 2016; Sasko et al., 2006) describe in detail the muscles responsible for closing the jaws and that integrate the mandibular abductor complex (the AMMAa, the AMLa and the AMMe). These muscles are large in size as compared to other species and the organization of the muscle bundle is adapted to the changes in size and thickening of the mandibular cartilages (González-Isáis, 2003; Kolmann et al., 2014, 2015). The detailed description of this muscular complex has been neglected in species whose feeding mode is nondurophagous; nevertheless, the data obtained from the three species described here exhibit important characteristics in the mandibular abductor complex, especially in *N. entemedor* due to the presence of their large mandibular cartilages to which the elongated AMMe, the excessive reduction of the AMLa and the compact organization of the medial muscle fibers of the AMMa are associated; suggesting that *N. entemedor* is a specialist in suction feeding, which is supported by the hypertrophied abductor muscles that generate large expansive forces in the mouth (Wilga et al., 2007). Beyond the evident and expected reduction of the adductor muscles, the presence of the anterior division of the AMMa, which is approximately half the size of the entire bundle and inserts on the surface of the antorbital cartilage, is noteworthy. The function of this section of AMMa is probably focused to increase the distance between the head and the substrate creating a higher space for the formation of a sucking tube during the "winnowing" phase of feeding, which was previously described by Dean and Motta (2004b) and consists of the continuous protrusion and retraction of the jaws with expulsion of inedible material.

The organization of the cranio-mandibular musculature of the species on this study is almost consistent with that previously described for other groups of batoids, since there is no thickening of the muscles responsible for jaw closure or the presence of a greater number of adductor bundles. In contrast, the presence of the rostral cartilage results from the presence of an additional muscle on the dorsal surface of the organisms (LR) and the reorganization of the insertion point of the antagonistic muscle (DR). However, the differences among the three species analyzed emphasized the type of prey they consume and the feeding strategies, *N. entemedor* is a suction specialist whose prey are mainly anguiliform organisms like polychaetes, nematodes and ascidians (Cabrera, 2017; Michael, 1993), as opposed to *R. velezi* and *Z. exasperata* whose feeding is mainly on larger organisms like fish, mollusks and small crustaceans (De la Cruz-Agüero et al., 1997; Grove & Lavenberg, 1997; Molina-Salgado et al., 2021). Further studies are necessary to develop descriptions of more batoid species to better understand the biology and feeding evolution of the batoid group.

AUTHOR CONTRIBUTIONS

Cristina Ramírez-Díaz: conceptualization; methodology; writing - original draft; investigation. **Renato Peña**: writing - original draft; conceptualization; writing - review & editing; investigation. **Rui Diogo**: writing - review & editing; validation. **Víctor H. Cruz-Escalona**: funding acquisition; project administration.

ACKNOWLEDGMENTS

This study was funded by the Consejo Nacional de Ciencia y Tecnología (CONACyT) project SEP-CONACyT 189894. C.R.D. is a

recipient of the Beca de Estímulo Institucional de Formación de Investigadores (BEIFI, Research Formation Incentives). R.P. and V.H.C.E. received fellowships from the Estímulo al Desempeño de los Investigadores (EDI; Research Performance Incentives) and the Comisión de Operación y Fomento de Actividades Académicas (COFAA; Commission for the Advancement of Academic Activities) of the National Polytechnic Institute of Mexico.

CONFLICTS OF INTEREST

The authors declare no conflicts of interest.

DATA AVAILABILITY STATEMENT

The data that support the findings of this study are available on request from the corresponding author.

ORCID

Renato Peña http://orcid.org/0000-0002-7559-585X
Rui Diogo http://orcid.org/0000-0002-9008-1910

REFERENCES

Aschliman, N. C., Nishida, M., Miya, M., Inoue, J. G., Rosana, K. M., & Naylor, G. J. P. (2012). Body plan convergence in the evolution of skates and rays (Chondrichthyes: Batoidea). *Molecular Phylogenetics and Evolution*, *63*, 28–42.

AVMA Panel on Euthanasia. American Veterinary Medical Association. (2001). 2000 Report of the AVMA panel on Euthanasia. *Journal of the American Veterinary Medical Association*, *218*(5), 669–696.

Cabrera, P. (2017). *Hábitos alimentarios de Narcine entemedor en la Bahía de La Paz, México*. [Unpublished doctoral dissertation] Centro Interdisciplinario de Ciencias Marinas, Instituto Politécnico Nacional. La Paz, BCS, Mexico, p. 79.

Collins, A. B., Heupel, M. R., Hueter, R. E., & Motta, P. J. (2007). Hard prey specialists or opportunistic generalists? An examination of the diet of the cownose ray, Rhinoptera bonasus. *Marine and Freshwater Research*, *58*, 135–144.

Dean, M. N., Azizi, E., & Summers, A. P. (2007). Uniform strain in broad muscles: Active and passive effects of the twisted tendon of the spotted ratfish *Hydrolagus colliei*. *Journal of Experimental Biology*, *210*, 3395–3406.

Dean, M. N., Wilga, C. D., & Summers, A. P. (2005). Eating without hands or tongue: Specialization, elaboration and the evolution of prey processing mechanisms in cartilaginous fishes. *Biology Letters*, *1*, 357–361.

Dean, M. N., & Motta, P. J. (2004a). Anatomy and functional morphology of the feeding apparatus of the lesser electric ray, *Narcine brasiliensis* (Elasmobranchii: Batoidea). *Journal of Morphology*, *262*, 462–483.

Dean, M. N., & Motta, P. J. (2004b). Feeding behavior and kinematics of the lesser electric ray, *Narcine brasiliensis* (Elasmobranchii: Batoidea). *Zool. 107*, 171–189.

De la Cruz-Agüero, J., Arellano-Martínez, M., Cota-Gómez, V. M., & De la Cruz-Agüero, G. (1997). *Catálogo de los peces marinos de Baja California Sur* (p. 346). IPN-CICIMAR.

Gerry, S. P., Summers, A. P., Wilga, C. D., & Dean, M. N. (2010). Pairwise modulation of jaw muscle activity in two species of elasmobranchs. *Journal of Zoology*, *281*, 282–292.

Gerry, S. P., Brodeur, L. K., DeCaprio, M., Khursigara, A. J., Mazzeo, S., & Neubauer, D. L. (2019). Jaw muscle activation patterns of several Batoids. *Environmental Biology of Fishes*, *102*, 1193–1200.

González-Isáis, M. (2003). Anatomical comparison of the cephalic musculature of some members of the superfamily myliobatoidea (chondrichthyes): Implications for evolutionary understanding: Cephalic Musculature of myliobatoids. *The Anatomical Record Part A: Discoveries in Molecular, Cellular, and Evolutionary Biology*, *271A*, 259–272.

González-Isáis, M., & Domínguez, H. M. M. (2004). Comparative anatomy of the superfamily Myliobatoidea (Chondrichthyes) with some comments on phylogeny: Comparative Anatomy of myliobatoids. *Journal of Morphology*, *262*, 517–535.

González Isáis, M., & Montes Domínguez, H. M. (2016). Compared morphology of the cephalic musculature in five species of genus Urotrygon (Chondrichthyes: Urolophidae). *International Journal of Morphology*, *34*(1), 7–12.

Gray, A. E., Mulligan, T. J., & Hannah, R. W. (1997). Food habits, occurrence, and population structure of the bat ray, *Myliobatis californica*, in Humboldt Bay, California. *Environmental Biology of Fishes*, *49*, 227–238.

Grove, J. S., & Lavenberg, R. J. (1997). *The fishes of the Galápagos Islands*. 863 p Stanford University Press.

Jacobsen, I. P., & Bennett, M. B. (2013). A comparative analysis of feeding and trophic level ecology in stingrays (Rajiformes; Myliobatoidei) and electric rays (Rajiformes; Torpedinoidei). *PLoS One*, *8*(8), e71348.

Kolmann, M. A., Huber, D. R., Dean, M. N., & Grubbs, R. D. (2014). Myological variability in a decoupled skeletal system: Batoid cranial anatomy. *Journal of Morphology*, *275*, 862–881.

Kolmann, M. A., Dean Grubbs, R., Huber, D. R., Fisher, R., Lovejoy, N. R., & Erickson, G. M. (2018). Intraspecific variation in feeding mechanics and bite force in durophagous stingrays. *Journal of Zoology*, *304*, 225–234.

Kolmann, M. A., Welch, Jr., K. C., Summers, A. P., & Lovejoy, N. R. (2016). Always chew your food: Freshwater stingrays use mastication to process tough insect prey. *Proceedings of the Royal Society B: Biological Sciences*, *283*, 20161392.

Kolmann, M. A., Huber, D. R., Motta, P. J., & Grubbs, R. D. (2015). Feeding biomechanics of the cownose ray, *Rhinoptera bonasus*, over ontogeny. *Journal of Anatomy*, *227*, 341–351.

Maisey, J. G. (1980). An evaluation of jaw suspension in sharks. *Amer. Mus. Novit. 2706*, 1–17.

McEachran, J. D., & Capape, C. (1984). Mobulidae. In (Eds.) J. C. Quero, J. C. Hureau, C. Karrer, A. Post & L. Saldanha, *Checklist of the Fishes of the Eastern Tropical Atlantic (CLOFETA)* (1, pp. 73–76). JNICT: Lisbon; SEI: Paris; Paris: UNESCO.

Michael, S. W. (1993). Reef sharks and rays of the world. A guide to their identification, behavior and ecology. *Sea Challengers, Monterey, California* (p. 107). Lighthouse Press.

Miyake, T., & McEachran, J. D. (1991). The morphology and evolution of the ventral gill arch skeleton in batoid fishes (Chondrichthyes: Batoidea). *Zoological Journal of the Linnean Society*, *102*, 75–100.

Miyake, T., McEachran, J. D., Walton, P. J., & Hall, B. K. (1992). Development and morphology of rostral cartilages in batoid fishes (Chondrichthyes: Batoidea), with comments on homology within vertebrates. *Biological Journal of the Linnean Society*, *46*, 259–298.

Molina-Salgado, P., Alfaro-Shigueto, J., & González-Pestana, A. (2021). Diet of the rasptail skate, Rostroraja velezi (Rajiformes: Rajidae), off Piura, Peru. *Ciencias Marinas*, *47*(2), 127–138.

Motta, P. J., & Huber, D. R. (2012). Chapter 6: Prey capture behavior and feeding mechanics of elasmobranchs. In (eds) J. C. Carrie, J. A. Musick & M. R. Heithaus, *Biology of Sharks and their relatives* (2nd ed., pp. 139–164). CRC Press.

Navarro-González, J., Bohórquez-Herrera, J., Navia, A., & Cruz-Escalona, V. (2012). Diet composition of batoids on the continental shelf off Nayarit and Sinaloa, Mexico. *Ciencias Marinas*, *38*, 347–362.

Nishida, K. (1990). Phylogeny of the order myliobatoidei. *Memoirs of the Faculty to Fisheries, Hokkaido University*, *37*, 1–108.

Notarbartolo-di-Sciara, G. (1987). A revisionary study of the genus Mobula Rafinesque, 1810 (Chondrichthyes: Mobulidae) with the

description of a new species. *Zoological Journal of the Linnean Society*, *91*, 1–91.

Paig-Tran, E. W. M., Kleinteich, T., & Summers, A. P. (2013). The filter pads and filtration mechanisms of the devil rays: Variation at macro and microscopic scales. *Journal of Morphology*, *274*, 1026–1043.

Sampson, L., Galván-Magaña, F., De Silva-Dávila, R., Aguíñiga-García, S., & O'Sullivan, J. B. (2010). Diet and trophic position of the devil rays *Mobula thurstoni* and *Mobula japanica* as inferred from stable isotope analysis. *Journal of the Marine Biological Association of the United Kingdom*, *90*(5), 969–976.

Sasko, D. E., Dean, M. N., Motta, P. J., & Hueter, R. E. (2006). Prey capture behavior and kinematics of the atlantic cownose ray, *Rhinoptera bonasus*. *Zoology*, *109*, 171–181.

Shibuya, A., Zuanon, J., & Tanaka, S. (2012). Feeding behavior of the neotropical freshwater stingray *Potamotrygon motoro* (Elasmobranchii: Potamotrygonidae). *Neotropical Ichthyology*, *10*(1), 189–196.

Simental, M. C. (2013). Ecología trófica de *Raja velezi* (Chirichigno, 1973), en la costa occidental de Baja California sur, México [Unpublished doctoral dissertation]. Centro Interdisciplinario de Ciencias Marinas, Instituto Politécnico Nacional.

Summers, A. P. (2000). Stiffening the stingray skeleton? an investigation of durophagy in myliobatid stingrays (Chondrichthyes, Batoidea, Myliobatidae). *Journal of Morphology*, *243*, 113–126.

Summers, A. P., & Koob, T. J. (2002). The evolution of tendon-morphology and material properties. *Comparative Biochemistry and Physiology Part A: Molecular & Integrative Physiology*, *133*, 1159–1170.

Svanbäck, R., Wainwright, P. C., & Ferry-Graham, L. A. (2002). Linking cranial kinematics, buccal pressure and suction feeding performance in large-mouth bass. *Physiological and Biochemical Zoology*, *75*, 532–543.

Weigmann, S. (2016). Annotated checklist of the living sharks, batoids and chimaeras (Chondrichthyes) of the world, with a focus on biogeographical diversity: Annotated global checklist of chondrichthyes. *Journal of Fish Biology*, *88*, 837–1037.

Whitenack, L. B., Kim, S. L., & Sibert, E. C. (2022). Chapter 1: Bridging the gap between chondrichthyan paleobiology and biology. In (Eds.) Carrier, J. C., Simpfendorfer, C. A., Heithaus, M. R., & Yopak K. E., *Biology of sharks and relatives* (3th Ed., pp. 1–29). CRC Press, Taylor & Francis Group.

Wilga, C. D. (2002). A functional analysis of jaw suspension in elasmobranchs. *Biological Journal of the Linnean Society*, *75*, 483–502.

Wilga, C. D. (2008). Evolutionary divergence in the feeding mechanism of fishes. *Acta Geologica Polonica*, *582*, 113–120.

Wilga, C. D., & Motta, P. J. (1998). Feeding mechanism of the atlantic guitarfish *Rhinobatos lentiginosus*: Modulation of kinematic and motor activity. *Journal of Experimental Biology*, *201*, 3167–3183.

Wilga, C. D., Maia, A., Nauwelaerts, S., & Lauder, G. V. (2012). Prey handling using whole-body fluid dynamics in batoids. *Zoology*, *115*, 47–57.

Wilga, C. D., Motta, P. J., & Sanford, C. P. (2007). Evolution and ecology of feeding in elasmobranchs. *Integrative and Comparative Biology*, *471*, 55–69.

How to cite this article: Ramírez-Díaz, C., Peña, R., Diogo, R., & Cruz-Escalona, V. H. (2022). Comparative cranio-mandibular myology of three species of Batoidea from the Southern Gulf of California, Mexico. *Journal of Morphology*, e21547. https://doi.org/10.1002/jmor.21547